Adsorption Behaviour of Cobalt onto Saline Soil with/without a Biosurfactant: Kinetic and Isotherm Studies

S. Narimannejad[a], B. Zhang[a,1], L. Lye[a]
[a] Faculty of Engineering and Applied Science, Memorial University of Newfoundland, St. John's, NL, A1B 3X5, Canada

Abstract

Cobalt (Co) adsorption onto saline soil was investigated in this study. The effect of pH, interaction time and initial concentration of Co on adsorption were evaluated empirically to screen the appropriate operating conditions. Three biosurfactant products (i.e., Surfactin, Trehalose lipids, Rhamnolipid) each at two concentrations (1 CMC and 2 CMC) were applied during Co adsorption. The adsorption kinetic models were explored and results indicated that the pseudo-second-order kinetic model fit the experimental data the best. Four isotherms, including Langmuir, Freundlich, Temkin and Redlich-Peterson were used for regulating the Co adsorption with and without the addition of each biosurfactant. The research results show that Co has low mobility even with the existence of a biosurfactant. The findings help to better understand the adsorption behaviour of Co in saline soil so as to develop applicable remediation options.

Keywords: Adsorption, biosurfactant, Co, isotherm, kinetics, saline soil

1 Introduction

Cobalt (Co) can enter the environment from natural sources and human activities, and occurs in different chemical forms. It can be released into the environment from burning coal and oil, incinerators, vehicular exhausts and industrial processes such as mining and operation of Co ores. To form a Co-base alloy, Co is blended with other metals. Alloys are resistant and used in industrial activities such as making aircraft, grinding and cutting tools (Altintas 2012). Exposure to Co can cause negative health effects such as asthma and pneumonia (Naqvi et al. 2008). The possibility of Co induced carcinogens in humans has been reported by the International Agency for Research on Cancer (WHO 2007).

Adsorption is the most important chemical process affecting the behaviour of heavy metals in a subsurface, and plays a key role in governing the mobility and fate of Co in soils (Jalali and Majeri 2016). Soil properties and acidic conditions affect Co adsorption behaviour (Faroon et al. 2004). A pH dependence experiment of Co sorption on soil displayed that Co sorption was strongly affected by the pH of a solution (Chon et al. 2012). The adsorption of Co from an aqueous solution strongly depended on pH so that, as the pH turned to alkaline range (pH equal to 9), soil adsorption capacity increased (Hashemian et al. 2015). Clay has a high capacity of metal adsorption comprising silt and sand, which makes Co removal from clay quite challenging. Moreover, soil salinity might impact the Co adsorption behavior; however, the impact has not been reported previously.

1. Corresponding author. Email address: bzhang@mun.ca. Tel.: +1 (709) 864-3301.

Adsorption dynamics, especially the kinetic models, have been used to track the associated mechanisms and to determine the adsorption rate of heavy metals in soil (Sheela et al. 2012). Pseudo-first and pseudo-second-order models were used to kinetically study Cu^{2+} adsorption in soil minerals (Komy et al. 2014). The kinetics of divalent copper and Co cations from aqueous solutions on clay samples demonstrated that the second-order model can better express the kinetics of both metal adsorptions (Guerra and Airoldi 2008). A nano hollow sphere was applied to remove heavy toxic metals (Hg^{2+}, Pb^{2+} and Cd^{2+}) from water samples. The sorption dynamics were established with the Lagergren pseudo-first-order, the pseudo-second-order and Elovich kinetic model (Rostamian et al. 2011). In order to predict adsorption the process of Co from aqueous solutions, pseudo-first-order and pseudo-second-order kinetic models were applied to the data (Hashemian et al. 2015). Study of kinetic models on the adsorption rate of Co^{2+} in activated carbon indicated that the system was described by the pseudo-second-order kinetic model (Abbas et al. 2014). Although there were many previous studies regarding heavy metal adsorption kinetics, limited works have targeted Co kinetics in the soil.

To achieve equilibrium data, isotherm studies are important for describing a solid-liquid adsorption system. Isotherms are an equilibrium relation between the adsorbate concentration in the solid phase and liquid phase (Sheela et al. 2012). Hashemian et al. (2015) demonstrated that the equilibrium data for Co adsorption had a high correlation coefficient when fitted with a Langmuir model. Jalali and Majeri (2016) found that the Co sorption could be well fitted with Langmuir and Freundlich models. Chon et al. (2012) disclosed that for sorption isotherm, there is a good fit with the Freundlich equation for the experimental results for Co sorption in soil. Chen and Lu (2008) indicated that the adsorption isotherm of Co on montmorillonite soil was linear at both pH values including 7.3 and 7.7. The experimental data fitted the Freundlich model. Guerra and Airoldi (2008) used a Langmuir isotherm model with a nonlinear approach and yielded good fits with the experimental adsorption data for divalent copper and Co cations/clay interactions. However, these studies only investigate systems with only Co and soil components. No studies have taken the impacts of other possible influences, such as soil washing agents, into the consideration.

Soil washing is a cost effective physio-chemical method to decontaminate the soil efficiently and a reliable metal removal alternative (Siddiqui et al. 2015). Because of wide applicability and economic feasibility, soil washing has played a major role and been successfully applied in the field (Ferraro et al. 2016). Co extraction can be carried out with different additives, such as acid solutions, reducing and oxidizing agents (Ferraro et al. 2016). During soil washing, solutions of surface-active molecules (i.e., surfactants) have been widely applied as washing agents (Harendra and Vipulanandan 2013). In recent years, biosurfactants have gradually replaced chemical surfactants in soil washing cases. Biosurfactants are promising due to their low toxicity, possibility of reuse and biodegradability (Cai et al. 2014). In heavy-metal contaminated soils, biosurfactants can form complexes with metals at the soil interface (Singh and Cameotra 2013). The process is followed by desorption of the metal and removal from the soil surface, leading to the increase of metal ions' concentration and their bioavailability in the soil solution. However, when using it to treat Co in the subsurface, the removal rate could be low. For example, soil washing aided by a biosurfactant (i.e., lipopeptide biosurfactant consisting of surfactin and fengycin) removed just 35.4% of Co from a contaminated soil (Singh and Cameotra 2013). Till now, there is a lack of literature regarding the impact of biosurfactants on Co adsorption in soil, and nearly no associated kinetics and isotherm studies have been reported.

To fill the knowledge gap, this study focuses on the investigation of Co adsorption on saline soil with and without the existence of the biosurfactant. Three biosurfactants, including surfactin, trehalose lipids and rhamnolipid products, were examined. The impact of pH, contact time, initial Co concentration, and type/dose of biosurfactant on Co adsorption were evaluated. Adsorption kinetics and isotherms were explored. The research results will help to better understand Co adsorption mechanisms in saline soil and Co-biosurfactant interaction during adsorption.

2 Materials and Methods

2.1 Soil Characterization

Soil including 50% natural clay and 50% sand was applied for conducting each experimental run. After removing gravel and rocks, the soil was dried and kept in an oven at 105° C overnight. The soil was then sieved to pass through a 1.18 mm opening size stainless-steel mesh (No. 16). The 3% saline soil was obtained through adding NaCl.

Soil physical properties, including pH (ASTM 2016a), soil bulk density (ASTM 2016b), and soil water content (ASTM 2016c) were characterized using standard methods. The soil cation-exchange capacity was measured using the protocol generated by Bower et al. (1952). The results are presented in Table 1.

Table 1 Soil physical properties

Soil properties		**Value**
Particle size distribution (%)	Clay (< 0.002 mm)	50
	Sand (< 1.18 mm)	50
Salt (%)		3
Water content (%)		13.79
Bulk density (g/cm^3)		1.97
pH (soil materials suspended in water)		7.91
pH (soil materials suspended in a 0.01 M calcium chloride solution)		7.68
pH (saline soil (3%) suspended in water)		7.59
pH (saline soil (3%) suspended in a 0.01 M calcium chloride solution)		7.35
CEC (cmol (+) / kg)		135

Major element oxides in the soil were determined by X-ray fluorescence (XRF) spectrometry analysis. Sand and clay in the soil were crushed using a mortar and pestle, then mixed together before testing. For each test, 20 mg of the mixture was used, with results shown in Table 2.

Table 2 Soil major element oxides

Element oxides	Na_2O Wt%	MgO Wt%	Al_2O_3 Wt%	SiO_2 Wt%	P_2O_5 Wt%	K_2O Wt%	CaO Wt%
Clay / Sand Mixture	1.42	2.52	12.74	47.98	0.1	2.99	3.04

Trace element concentrations in the soil were obtained using inductively coupled plasma mass spectrometry (ICP-MS), with results presented in Table 3. Before analysis, sample preparation was conducted through a full digest of each sand/clay mixture.

Table 3 Soil trace element concentrations

Element	Value (ppm)	Element	Value (ppm)	Element	Value (ppm)	Element	Value (ppm)
Li	9.22	Cs	1.13	Nd	28.6	Dy	6.35
Rb	48.4	Ba	621	Sm	6.53	Ho	1.32
Sr	351	La	22.94	Eu	1.93	Er	3.76
Y	35.1	Ce	51.0	Gd	7.01	Tm	0.542
Zr	194	Pr	6.84	Tb	1.03	Yb	3.43
Lu	0.520	Tl	0.244	Pb	9.70	Pb	9.70

2.2 Biosurfactant Production

2.2.1 Biosurfactant-Producing Microorganisms

Three different lab-generated biosurfactants were applied. The impact of each biosurfactant on Co adsorption in soil was evaluated. Two types of the biosurfactants were generated in the Northern Region Persistent Organic Pollution Control (NRPOP) Laboratory at Memorial University of Newfoundland. The first one was produced by *Bacillus subtilis* N3-1P isolated from oily seawater (Cai et al. 2014). The product, Surfactin, is a lipopeptide biosurfactant which can reduce water surface tension significantly (Zhu et al. 2016). The hyper-production strain, Rhodococcus erythropolis Mutant M36, was obtained through UV mutagenesis of a wild strain isolated from produced water samples from offshore Newfoundland, Canada (Cai et al. 2016) and used to generate the second biosurfactant product containing trehalose lipids. The third biosurfactant applied in this study was crude rhamnolipid produced by a research partner's lab.

2.2.2 Biosurfactant Production by *B. Subtilis* N3-1P

The recipe for preparing the agar plate to grow B. subtilis N3-1P was as follows: Tryptic Soy Broth 30.0 g, NaCl 15 g and Agar Bacteriological 15 g in 1 L of distilled water. BD Difco™ Nutrient Broth 23400 (Fisher Scientific Company, Ottawa, Canada) 8.0 g and NaCl 5.0 g in 1 L of distilled water is used as the recipe for a inoculum broth (Zhu et al. 2016).
A loopful of bacteria was transferred from the agar plate to a 50-mL inoculum broth in a 125-mL Erlenmeyer flask. At first the culture in the flask was grown on a rotary incubator shaker (Thermo MaxQ 4000) at 200 rpm for 48 h at room temperature. The culture was applied as inoculum at the 1% (v/v) level. This means that 1 cc of the culture was used for biosurfactant production in the 100 cc mineral salt medium.

An improved mineral salt medium (MSM) for *B. subtilis* N3-1P fermentation (Zhu et al. 2016) was listed as follows (g / L): glycerol (10), nitrogen source $(NH_4)_2SO_4$ (10), NaCl (15), $FeSO_4$

$7H_2O$ (2.8×10^{-4}), KH_2PO_4 (3.4), K_2HPO_4 $3H_2O$ (4.4), $MgSO_4$ $7H_2O$ (1.02), yeast extract (0.5) and trace element solution 0.5 mL L^{-1} of distilled water. The composition of the trace element solution was as follows: $ZnSO_4$ (0.29), $CaCl_2$ (0.24), $CuSO_4$ (0.25), and $MnSO_4$ (0.17) g per 1 L of distilled water. It should be noted that the trace element solution was sterilized separately. In this growth media, the carbon source in the original recipe, glycerol (GLY), was changed by glucose (GLU) and sucrose (SUC) at a concentration of 15 g/L each. Also Nitrogen sources ($(NH_4)_2SO_4$)) were replaced by NH_4NO_3 at a concentration of 10 g/L. The original concentration of $FeSO_4$ $7H_2O$ was changed to 0.001 g/L.

Fermentation of *B. subtilis* N3-1P took place in a sterilized fermenter containing 2 L MSM and inoculum at the 1% (v/v) level. The medium was incubated in the fermenter at 400 rpm for 7 days at 30˚C. To remove all the cells, the culture broth was centrifuged at 6,000 rpm for 20 min. Then the pH of the biosurfactant solution was adjusted to 2 using concentrated hydrochloric acid. The solution was kept in a cooler overnight so biosurfactant precipitated in the container. The biosurfactant was separated in the centrifuge at 4,000 rpm for 15 min. The produced biosurfactant was washed with dichloromethane (DCM) for further purification and left in the hood overnight. The powdered biosurfactant product was transferred to the freezer to prevent degradation.

2.2.3 Biosurfactant Production by *Rhodococcus Erythropolis Mutant M36*

To prepare agar plates to grow *Rhodococcus erythropolis* Mutant M36, BD Difco™ Nutrient Broth 23400 (Fisher Scientific Company, Ottawa, Canada) 8 g, NaCl 20 g and agar bacteriological 15 g were dissolved in 1 L of distilled water. The composition of the medium used for fermentation of the mutant was as follows (g/L): glycerol (1), NaCl (10), $MgCl_2$ (0.1), $CaCl_2$ (0.1), $FeCl_3$ (0.01), NH_4NO_3 (1), KH_2PO_4 (0.41), K_2HPO_4 (8.2) and Diesel 100 mL L^{-1} of distilled water.

Before the fermentation, the medium and the fermenter were both sterilized by autoclaving. The strains from the prepared agar plate were transferred into the medium, which was incubated in the magnetic shaker for 5-7 days. During the first 2 days, the temperature of the shaker was adjusted to 30˚C. Afterwards, room temperature was used.

After the fermentation, the culture broth was transferred to a separation beaker and the water phase was discarded. To remove diesel, an equal volume of petroleum ether was added and the mixture was centrifuged at 4,000 rpm for 10 min. Then, the upper layer was discarded using a pipette. The diesel removal treatment was repeated 3 times to obtain a diesel-free product. The mixture containing biosurfactant was further purified through organic solvent extraction with a fivefold volume of methanol-chloroform (1:2 *v/v*) solvent. The solution was sonicated with an intensity level of 30% for 20 min. To remove the cells, the solution was centrifuged at 6,000 rpm for 20 min. The crude biosurfactant was concentrated by rotary evaporation and the final jelly product was frozen at 0˚C.

2.3 Co Adsorption onto Soil without Biosurfactant Addition

Co adsorption onto saline soil under various pH, initial Co concentrations and durations was conducted. Table 4 lists the number of runs when one-factor-at-a-time approach was used.

Table 4 Experimental runs and associated conditions

Effect of factor	Number of levels	Replication	Number of blanks	Replication	Total number of runs
pH	8	3	1	3	27
Time	12	3	12	3	72
Initial Co concentration	6	3	1	3	21

2.3.1 Effect of pH on Co Adsorption

The soil was air dried, homogenized, and kept in an oven at 105˚C for 1 day. Each 2.9 g sample of 3% saline soil was equilibrated in a polypropylene centrifuge tube with 50 ml of solution including a 300 mg/L concentration of Co.

Samples before adsorption experiments were adjusted to a pH range of 3 to 9 (including pH 3, 4, 5, 6, 7, 7.5, 8, 9) by 1 M HCI or 1 M NaOH solution. During each adsorption run, the pH measurement was carried out. The pH level of each run was kept consistent by adding small volumes of 0.1 M HCI or 0.1 M NaOH solution. Blank runs were prepared without the adjustment of soil pH levels. Distilled water was applied instead of the Co solution during each blank run. Co adsorption was carried out by shaking each tube in a shaker at 200 rpm and at the room temperature for 48 hours. After reaching the ultimate equilibrium status, the tube was centrifuged at 12,000 rpm for 20 min. The supernatant was acidified to pH 2 using 2% HNO_3 for flame atomic absorption spectroscopy (FAAS) measurement and the Co concentration remaining in the solution after each adsorption treatment was determined. A calibration curve for Co was constructed using standard solutions. Differences between each initial Co concentration in the solution and the remaining Co concentration in the supernatant after sorption indicated amount of Co that was adsorbed by the soil.

2.3.2 Effect of Adsorption Time

Adsorption was also carried out with 2.9 g saline soil and 50 mL of Co solution with the initial Co concentration of 300 mg/L. The effect of reaction time on Co adsorption was investigated at room temperature and the pH level selected based on a previous pH examination experiment.

The equilibration status of each run was investigated when shaking the tube at 200 rpm for various (i.e., 0, 10, 60, 120,180, 240, 300, 360, 420, 480, 540 and 600 min) times. Triplicate runs were conducted for each experimental setting. After adsorption, each tube was centrifuged at 12000 rpm for 20 min and the Co concentration remaining in the solution was measured using FAAS. In each blank run, no pH adjustment was conducted and no Co was added to the soil.

2.3.3 Effect of Initial Co Concentration

Various concentrations of Co solution (i.e., 50 ppm, 100 ppm, 200 ppm, 250 ppm, 300 ppm and 400 ppm) were applied to investigate the consequences of initial Co concentration on adsorption. Each Co adsorption run was carried out with 2.9 g saline soil, at room temperature and the pH

level selected based on previous pH examination experiments. During each run, the tube was shaken at 200 rpm to allow efficient mixing of the Co throughout the solution. After adsorption, each tube was centrifuged and aliquots of the supernatant solutions were taken for FAAS analysis. In each blank run, no pH adjustment was conducted and no Co was added to the soil. Triplicate runs were conducted for each experimental setting.

2.4 Co Adsorption onto Soil with Biosurfactant Addition

Solutions with different Co concentrations (i.e., 50 ppm, 100 ppm, 200 ppm, 300 ppm and 400 ppm) were prepared. Three different types of biosurfactant products were applied at two concentrations (1 and 2 CMC), respectively. Co adsorption onto soil with added biosurfactant was examined using runs, indicated in Table 5.

Table 5 Number of runs

Biosurfactant	Concentration	Number of levels	Replication	Total number of runs
Surfactin	1 CMC	5	3	15
Surfactin	2 CMC	5	3	15
Trehalose lipids	1 CMC	5	3	15
Trehalose lipids	2 CMC	5	3	15
Rhamnolipid	1 CMC	5	3	15
Rhamnolipid	2 CMC	5	3	15

In each experimental run, 2.9 g of saline soil was placed into a 50 mL centrifuge tube. The Co solution was added to the tube followed by the addition of a biosurfactant product. The pH of the suspensions was adjusted to the desired level based on previous a pH examination experiment. Each tube was shaken in a shaker at 200 revolutions per minute at room temperature. The adsorption duration was selected based on previous examination, as stated in section 2.3. Once reaching equilibration status, each tube was centrifuged and the supernatant solutions were engaged for FAAS analysis to obtain the Co concentration in the solution after adsorption. Surface tension analysis was applied to define the biosurfactant concentration in the supernatant solution. Both Co and biosurfactant adsorption in the soil were examined. In each blank run, pH adjustment was conducted and no biosurfactant was added to the soil. Triplicate runs were conducted for each experimental setting.

2.5 Biosurfactant Adsorption onto Soil without Existence of Co

To measure biosurfactant adsorption, 2.9 g of saline soil was placed into 50 mL centrifuge tubes. The soil was suspended in 50 mL of varying concentrations (1 and 2CMC) of 3 different types of biosurfactants (Table 6). Blank solutions contained the soil solution without the addition of any biosurfactant.

Table 6 Number of runs

Biosurfactant	Concentration	Replication	Total number of runs
Surfactin	1 CMC	3	3
Surfactin	2 CMC	3	3
Trehalose lipids	1 CMC	3	3
Trehalose lipids	2 CMC	3	3
Rhamnolipid	1 CMC	3	3
Rhamnolipid	2 CMC	3	3

The contact time and pH levels were selected based on the results of section 2.3. Each tube was incubated in a shaker at 200 rpm at room temperature. After reaching the ultimate equilibrium, the tube was centrifuged at 12,000 rpm for 20 min. Biosurfactant concentration in the supernatant was measured using surface tension analysis. The Du Nouy ring method of measuring surface tension was applied to measure surface tension.

2.6 Kinetic Studies of Co Adsorption to Soil without Existence of Biosurfactants

The capacity of sorption q_t (mg g^{-1}) of soil was computed using (Najafi et al. 2011):

$$q_t = ((C_0 - C_t)/ w) \,.\, V \quad (1)$$

where C_0 is the initial Co concentration (mg L^{-1}), C_t is the residual metal concentration (mg L^{-1}) at time t, V is the volume of Co solution (L), and W is the amount of soil (g). To present the Co sorption kinetics in the soil, pseudo-first-order, pseudo-second-order, Elovich and intra-particle diffusion kinetic models were examined. The linearized form of the pseudo-first-order equation (Lagergren) was stated as follows (Arabloo et al. 2016):

$$\ln (q_e - q_t) = \ln (q_e) - k_1 t \quad (2)$$

where q_e and q_t are the adsorption capacity at equilibrium and at any time t, respectively (mg_{Co} g_{soil}^{-1}), and the value of k_1 (min^{-1}) is the rate constant of pseudo-first-order adsorption. The differential formula for the pseudo-second-order rate model was expressed as (Smiciklas et al. 2008):

$$t/q_t = (1/k_2 q_e^2) + (1/q_e)\, t \quad (3)$$

where the value of k_2 (g $mg^{-1}min^{-1}$) is the overall rate constant of the pseudo-second-order adsorption rate constant. The simplified form of the Elovich equation was presented as follows (Pérez-Marín et al. 2007):

$$q_t = 1/ß \ln (\alpha ß) + 1/ß \ln (t) \quad (4)$$

where α is the initial adsorption rate constant (mg/g min) and ß is a measure of adsorption activation energy (g/mg). The possibility of intra-particle diffusion was expressed as (Sheela et al. 2012):

$$q_t = k_{id}\, t^{0.5} + I \quad (5)$$

where k_{id} is the intraparticle diffusion rate constant (mg/g $min^{0.5}$) and I is the thickness of film.

2.7 Isotherm Examination of Co Adsorption to Soil with and without Existence of Biosurfactants

To determine the adsorption isotherms, the graph relating equilibrium Co concentration and mass of Co adsorbed on per unit mass of the soil interface at a fixed temperature and pH was employed. The quantity of metal sorbed was calculated as the difference between the initial (C_0; mg/L) and final or equilibrium solution concentrations (C_e; mg/L). By using a mass balance equation, the mass of metal adsorbed by the soil ($q_{e;}$ mg/g_{soil}) was calculated in every test tube as follows:

$$q_e = v/m\,(C_0 - C_e) \quad (6)$$

where v is the volume of the solution used (mL) and m is the dry mass of soil used (mg).

The equilibrium experimental data were examined using 4 most commonly used adsorption isotherms, including Langmuir, Freundlich, Temkin and Redlich-Peterson, for Co isotherm investigation. When the extent of coverage of adsorbate was restricted to only one molecular layer, the Langmuir isotherm was applicable (Arabloo et al. 2016). The associated isotherm equation was expressed by Eq. 7:

$$q_e = Q_0 K_L C_e / 1 + K_L C_e \quad (7)$$

Here and in all isotherms analyzed, q_e (mg/g) is the amount of adsorbed Co per unit weight of the soil and C_e is the equilibrium Co concentration in the solution. K_L (L/mg) is the constant of the adsorption equilibrium and Q_0 (mg/g) is the maximum amount of adsorbed Co per unit weight of the soil. The empirical Freundlich model was generated based on multilayer adsorption on a heterogeneous surface (Arabloo et al. 2016). The model was stated by the following equation:

$$q_e = K_F\, C_e^{1/n_f} \quad (8)$$

where K_F is adsorption capacity and n_f is adsorption intensity (heterogeneity factor).

The Temkin model, similar to the Freundlich isotherm, was used to present the increased linearly of the solid surface area with decreased adsorption heat (Arabloo et al. 2016). The Temkin model was first developed for investigating a solid/gas system, and then extended its applications to the solid/liquid system. Tong et al. (2011) applied the Temkin isotherm for modeling adsorption of copper ion's to a solid sorbent from an aqueous solution. Siva Kumar et al. (2012) conducted equilibrium studies on biosorption of 2, 4, 6-trichlorophenol from aqueous solutions with Acacia leucocephala bark using the Temkin isotherm. The Temkin isotherm was expressed through the following form:

$$q_e = (RT / b_T) \ln A_T\, C_e \quad (9)$$

where B = RT / b_T and is related to the heat of adsorption. A is the equilibrium binding constant related to the maximum binding energy (Rostamian et al. 2011).

A further empirical model, Redlich and Peterson's, was also adopted. It is a three-parameter adsorption isotherm and a combination of elements from Langmiur and Freundlich equations. This model does not follow ideal monolayer adsorption and the adsorption mechanism is a hybrid (Rostamian et al. 2011). The model was expressed as:

$$q_e = (K_R C_e) / (1 + a_R C_e^g) \quad (10)$$

where g, K_R (L/g), a_R (mg^{-1}) are the exponent, Redlich-Peterson isotherm constant and constant, respectively. When $a_R C_e^g$ is bigger than 1, the model befits the Freundlich equation. When $a_R C_e^g$ is smaller than 1, it fits a linear equation that occurs at low concentrations (Aşçi et al. 2007).

2.8 Sample Analysis

The pH measurement was conducted by using a meter from METTLER TOLEDO Co. The electrical conductivity (EC) of samples was measured by a portable meter (VWR). A flame atomic absorption spectrometer (FAAS) (Varian, version 1.133) was employed to determine the Co concentration of samples. Inductively coupled plasma mass spectrometry, ICP-MS (PerkinElmer Elan DRC II ICP-MS), was used to measure the elements in the soil as a background.

Surface tension (ST) was measured with a 20 mL solution by the ring method using a Du Nouy Tensiometer (CSC Scientific). The critical micelle concentration (CMC) is the concentration of biosurfactant at which micelle starts to form (Mulligan et al. 2001). Surface tensions of lab generated biosurfactants as a function of concentration of biosurfactant were plotted. The CMC of each biosurfactant was obtained from the intercept of two straight lines extrapolated from the concentration-dependent and concentration-independent parts (Freitas de Oliveira et al. 2013). The CMC of three biosurfactants, including surfactin, trehalose lipids and rhamnolipid products, were 0.09 g/L, 3 ml/L (2.6 g/L) and 7 ml/L (7.05 g/L), respectively. The two biosurfactants produced in the NRPOP Laboratory were obtained from the most robust isolates/mutants screened in our previous studies (Cai et al., 2014; Cai, 2018). The CMCs of these biosurfactants are competent when compared with those in the previous studies.

The sorption model constants were estimated from sorption data of Co on the soil using MATLAB (R2017a version) and Excel (2016) computer programs. All of the tests were quoted using the mean ± standard division of the triplicated data and the typical error in the measurement was less than ±5%. The statistical analyses agreed to within 95% confidence demonstrating the accuracy of measurements reported in this study.

3 Results and Discussion

3.1 Co Adsorption onto Soil without Biosurfactant Addition

3.1.1 Impact of pH on Co Adsorption

Previously studies were conducted to select the appropriate pH of an aqueous solution for achieving the maximum adsorption of metal ions, including Cu, Cd, and Zn, onto the adsorbent (Ebrahimzadeh Rajaei et al. 2013; Filipkowska and Kuczajowska-Zadrozina 2016; Meitei and Prasad 2013). In this study, the pH values of Co solutions were varied over the range of 3 to 9 to assess the impact of pH on Co adsorption. Results indicated that Co adsorption by soil increased with increasing pH at a constant initial concentration of Co (300 mg/L) in all solutions. Therefore, the Co concentration in each solution at the equilibrium status decreased with increasing pH (Fig.1). Reduction of the pH value to 3.0 led to Co adsorption by 77 mg/L. A pH 9 was selected in further experiments since it helped to achieve the maximum Co adsorption in the system.

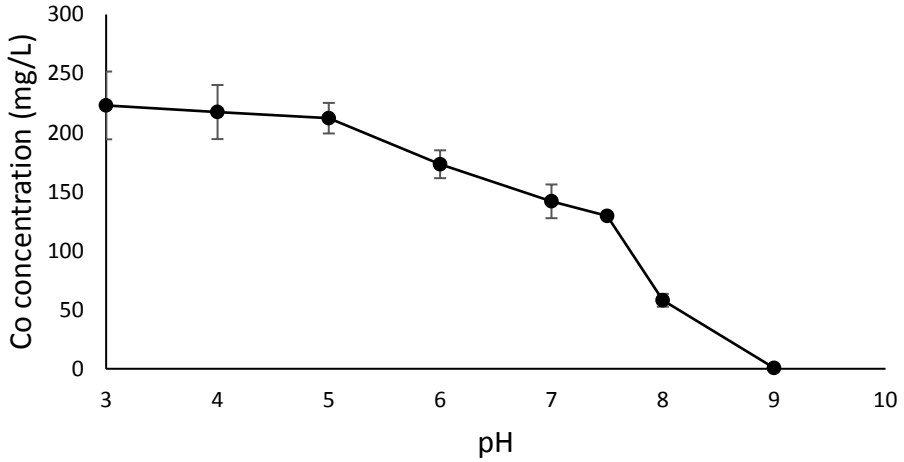

Fig. 1 Co adsorption depending on the pH

3.1.2 Impact of Time on Co Adsorption

Fig. 2 presents the mass of Co adsorbed onto the soil particles. The bulk of the Co sorbed by soil increased significantly within 120 minutes. Consequently, the rate of Co uptake slowed down gently as available adsorption sites were occupied by the metal ions. The result is well aligned with work conducted by Srivastava et al. (2006). After 420 minutes, the maximum Co adsorption was achieved and Co concentration in the solid phase became stable. The adsorption time (i.e., 420 min) was thus selected for conducting the following experiments.

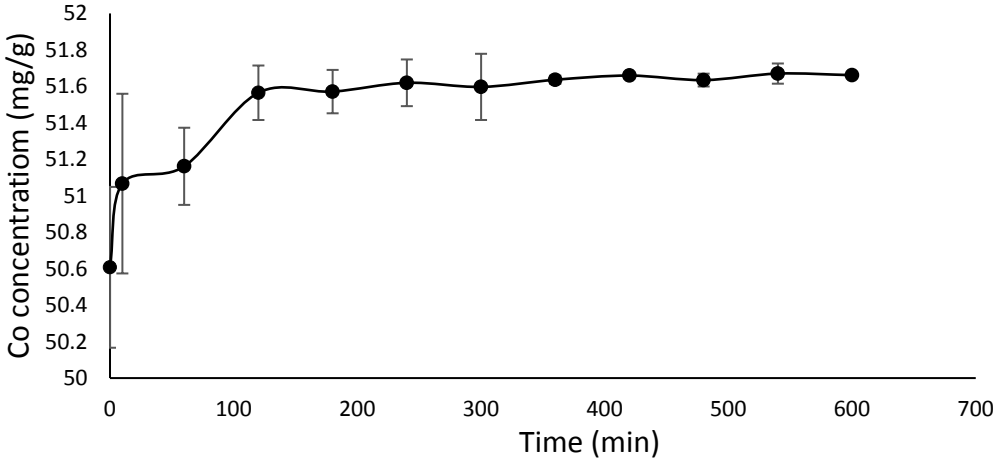

Fig. 2 Effect of contact time on Co adsorption by soil

3.1.3 Impact of Initial Concentration of Co on Adsorption

The impact of initial Co concentration in the solution on the capacity of Co adsorption onto soil is illustrated in Fig. 3. The amount of Co ions adsorbed onto soil at equilibrium status increased with raising the initial Co concentration in the solution.

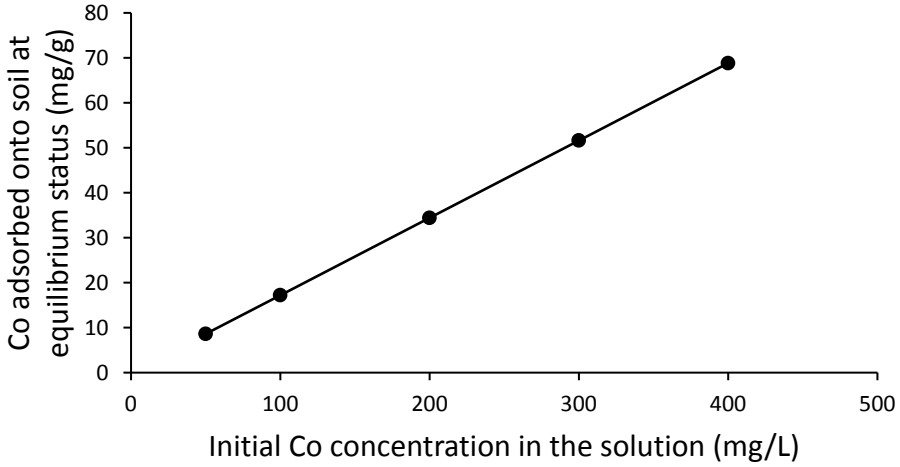

Fig. 3 Effect of initial concentration on Co adsorption

3.2 Biosurfactant Adsorption onto Soil without Existence of Co

Once biosurfactant molecules are adsorbed to the soil surface, the associated capacity for forming complexes with Co decreases. To evaluate the adsorption capacity of each type of biosurfactant during its application, experiments without the existence of Co were conducted. One and two

CMCs of each type of biosurfactant were adopted as initial concentrations before adsorption. After each adsorption run, the surface tension of each solution was tested, with results presented in Table 7. Under both experimental settings (i.e., 1 CMC and 2 CMC), the resulting surface tension values with the addition of Surfactin were lower than for those runs with Rhamnolipid. The use of Trehalose lipids led to much higher surface tension values after adsorption compared with the other two types of biosurfactant.

The surface tension values of the 1CMC solutions of three Surfactin, Trehalose lipids and Rhamnolipid are 32 mN/m, 33 mN/m and 40 mN/m, respectively. For Surfactin, after adsorption treatment, the surface tension was nearly unchanged, which indicated that Surfactin has an extremely limited adsorption capacity in a soil-water system. The finding delivered the information that Surfactin might be a good candidate for soil washing treatment due to its low adsorption capacity. However, the surface tension of Trehalose lipids was sharply increased after adsorption, showing that the molecules could easily adsorb to the soil surface. The high sorption capacity of a biosurfactant would lead to its low availability for metal complexation (Aşçi et al. 2007).

Table 7 Measured ST of solution after biosurfactant adsorption

Initial biosurfactant concentration	Surfactin ST	Trehalos lipid ST	Rhamnolipid ST
0 CMC (Blank)	72	72	72
1CMC	32.7	70	63.4
2CMC	32.5	69.5	57.6

3.3 Co Adsorption onto Soil with Biosurfactant Addition

The presence of surfactant in soil may affect Co adsorption. By adding various concentrations of each biosurfactant to soil, the pattern of Co adsorption changes. The blank experiments were conducted by adsorbing Co onto soil with different Co initial concentrations (i.e., 50 ppm, 100 ppm, 200 ppm, 300 ppm and 400 ppm) without the addition of any biosurfactant. The results of blank experiments are shown in Fig. 4.

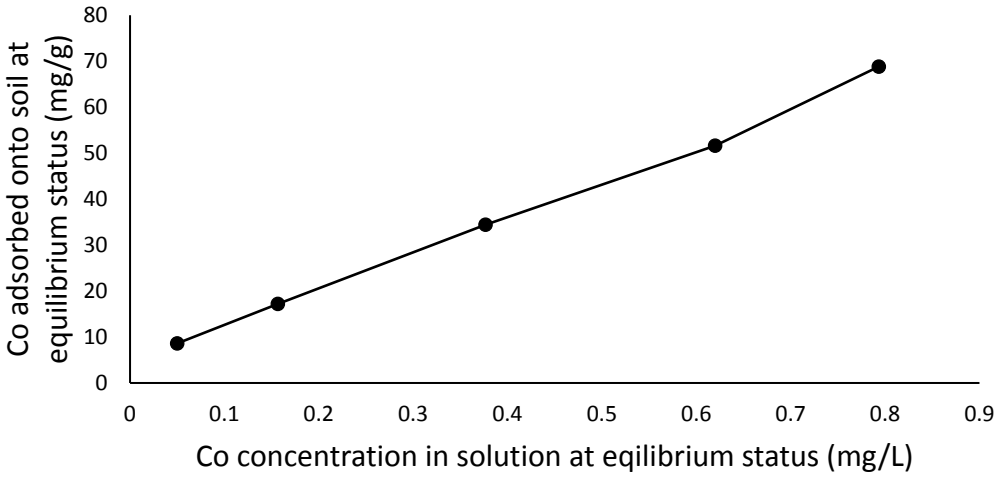

Fig. 4 Co adsorption by soil without the addition of any biosurfactant

Fig. 5 indicates the Co adsorption onto soil with the addition of 1 CMC and 2 CMC of the biosurfactant produced by B. subtilis N3-1P. At lower initial concentrations of Co (i.e., 50 ppm and 100 ppm), the Co equilibrium concentration in the solution is higher in each system with 2 CMC of the biosurfactant addition than that with 1 CMC of the biosurfactant. Once the initial concentration of Co increased to 200 ppm or even 400 ppm, both the Co equilibrium concentration in the solution and the associated Co adsorbed onto soil remained the same when comparing a system with 2 CMC of the biosurfactant's addition to that with 1 CMC of the biosurfactant. Co can be adsorbed onto the surface of soil particles and also react with the biosurfactant to form a complex. The complex can be adsorbed by the soil particles as well. Results illustrate that a higher biosurfactant concentration (i.e., 2 CMC) with lower initial Co concentrations (i.e., 50 ppm, 100 ppm) led to a bit less Co being adsorbed. This might be due to a higher competition of surface area of soil particles between the Co and biosurfactant molecules. Once the initial concentration of Co became higher (i.e., 200 ppm, 300 ppm and 400 ppm), Co molecules had a higher competitive capacity for reaching the surface area of soil particles, which resulted in the stable Co adsorption status after equilibrium in both types of systems (with 1CMC and 2 CMC of the biosurfactant).

Fig. 6 presents the change of surface tension in the solution after adsorption versus the initial concentration of Co. At a low initial concentration (i.e., 50 ppm and 100 ppm), the surface tensions in the 1 CMC system are slightly higher than those in the 2 CMC system. In addition, the surface tension values in both systems (i.e., 1 CMC and 2 CMC) are relatively low, which means there are still many free biosurfactant molecules after forming complexes with Co in the solution after adsorption. Once the initial Co concentration was increased to 300 ppm or even 400 ppm, the ratio of the number of Co ions to the number of biosurfactant molecules decreased in both experimental settings. The surface tension values in the solutions for both settings (i.e., 1 CMC and 2 CMC) are quite similar (reaching the surface tension of water) because all free biosurfactant molecules have either been used to form a complex with Co or are attached to the soil surface.

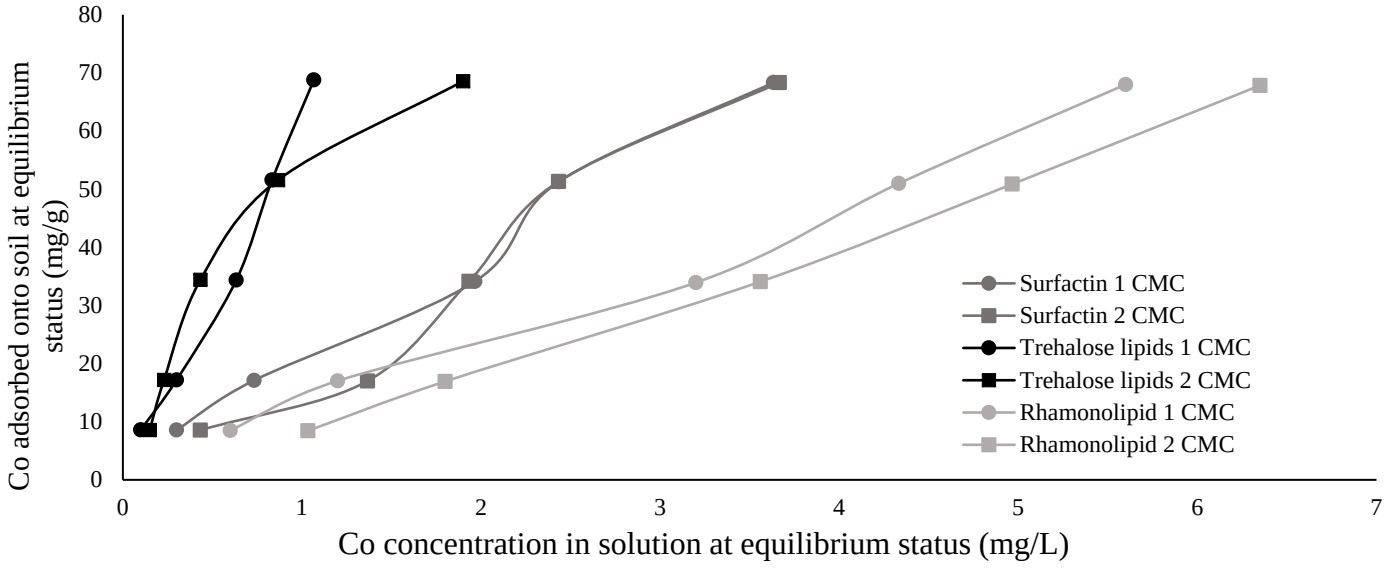

Fig. 5 Co adsorption by soil by applying 1 CMC and 2 CMC of biosurfactant

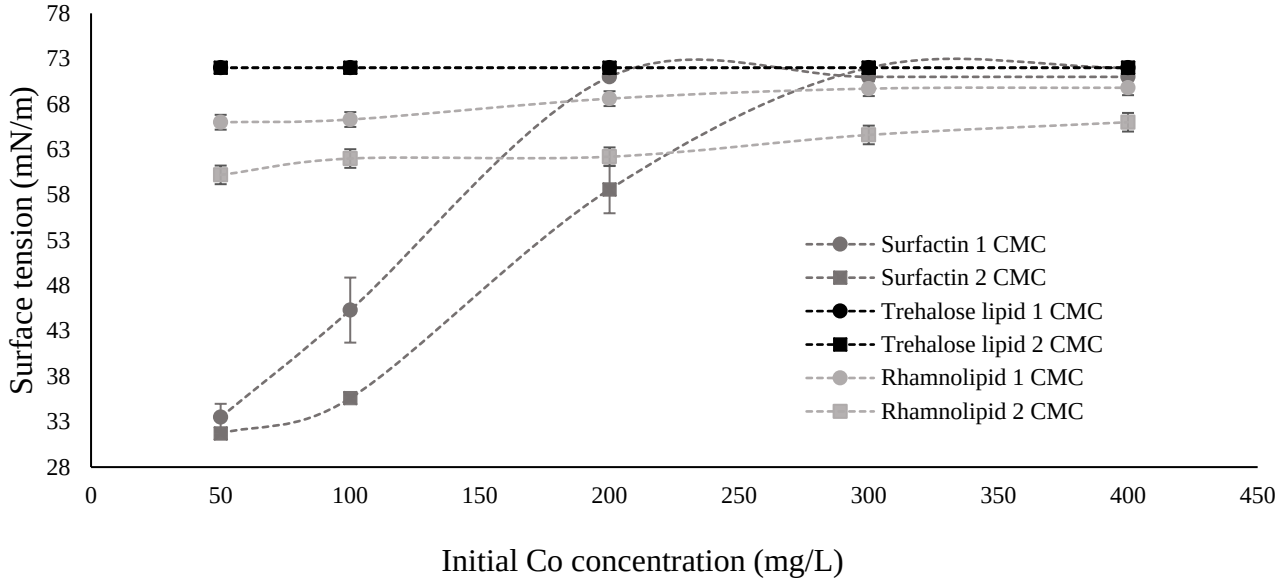

Fig. 6 Surface tension measured at 1CMC and 2CMC of biosurfactant after adsorption

The examination of Co adsorption onto soil with the addition of the second type of biosurfactant, trehalose lipids produced by *Rhodococcus* M36, was conducted with all experimental settings the same as the previous ones with surfactin. Both 1CMC and 2 CMC of the trehalose lipids were applied and the results are presented in Figs. 5 and 6. Fig. 5 indicates that the trehalose lipids' addition resulted in lower remaining Co concentrations in the solutions than those in the matrix with surfactin. Table 7 indicates that the trehalose lipids biosurfactant has a higher capacity to be adsorbed by the soil. The surface tensions of those solutions after adsorption are also much higher (Fig. 6) due to the sorption of biosurfactant in the soil which causes lower soil surface availability for Co ions. Additionally, Co could adsorb to the soil particles and also make a complex with biosurfactants. Consequently, the surface tension declines when the trehalose lipids biosurfactant transfers from its original form to the complex form. The amount of remaining Co in solution with trehalose lipids falls sharply compared with surfactin. With a high biosurfactant concentration (2 CMC), the remaining Co concentrations are slightly different than those with a low biosurfactant concentration (1 CMC), except for the last data, which almost doubled (rising from 1.06 mg/L in the 1CMC biosurfactant system to 1.9 mg/L in the 2 CMC biosurfactant one).

Rhamnolipid at 1 CMC and 2 CMC concentrations was also applied. In both systems, the increase of initial Co concentration resulted in the increase of Co concentration in the solution at the equilibrium status (Fig. 5). The addition of rhamnolipid at 2 CMC led to a higher equilibrium Co concentration compared to the results of the 1 CMC rhamnolipid system. In addition, the addition of rhamnolipid resulted in higher equilibrium Co concentrations in general when compared to the addition of the other two types of biosurfactants.

Fig. 6 indicates the surface tension in each solution after adsorption versus the Co initial concentration. The surface tensions at 1 CMC biosurfactant concentration are slightly higher than those at 2 CMC biosurfactant concentration. The surface tension varies between 60-70 (mN/m). The rhamnolipid shows a high tendency of being adsorbed to the soil (Table 7).

3.4 Kinetic Studies of Co Adsorption to Soil without Existence of Biosurfactants

Adsorption kinetics describe the uptake rate of Co onto the soil particles. Fig. 7 shows how the pseudo-first-order kinetic fits the experimental data. The values of $k_1$and q_e are determined by using the intercept and slope of the linear plot of ln ($q_e - q_t$) versus t. The determined R^2 and k_1 values are 0.8427 and 0.0078, respectively.

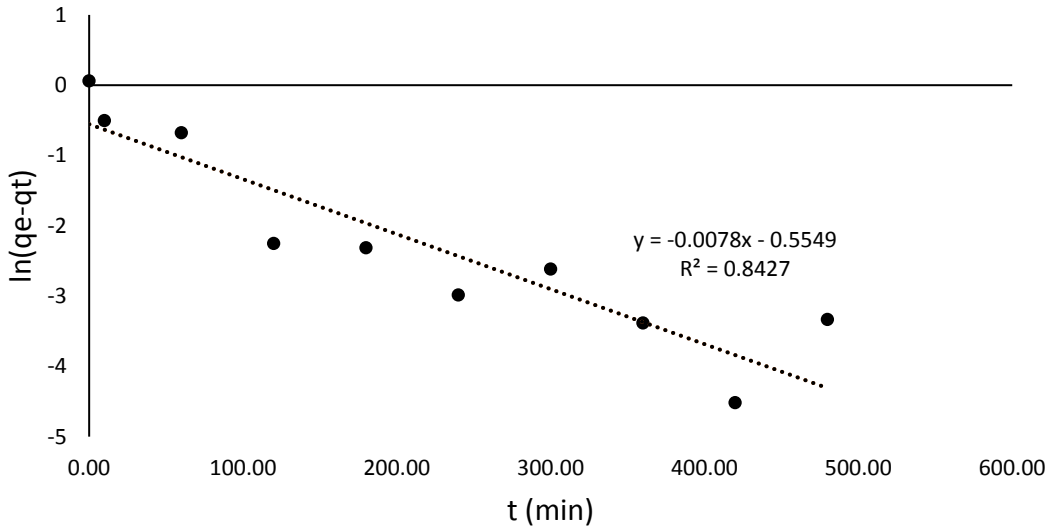

Fig. 7 Pseudo-first-order adsorption kinetic of Co onto the soil

To determine the values of q_e and k_2 in the pseudo-second-order model, the intercept and slope of the linear plot of t/q_t against t were applied (Fig. 8). The k_2 value calculated is equal to 0.0677. The coefficient of determination (R^2 value: 1) proves the reliability of the pseudo-second-order to explain the Co adsorption kinetic onto the soil. The high R^2 value obtained and the calculated Co equilibrium concentration ($q_{e\text{-}cal}$ equal to 51.8134 mg/g) show that the pseudo-second-order could be a better model to designate the kinetic of the process. The Co equilibrium concentration obtained from experiments q_e is 51.6591 mg/g. According to R^2 and $q_{e\text{-}cal}$, the pseudo-second-order model suggests that the rate limiting step in divalent metal sorption on the soil involves valence forces through exchange or a sharing of electrons between the sorbates and sorbent (Ho and McKay 1999). Thus, the significant correlation between experimental data and this kinetic model is helpful for q_e prediction and comparison regarding Co adsorption (Coleman et al. 2006).

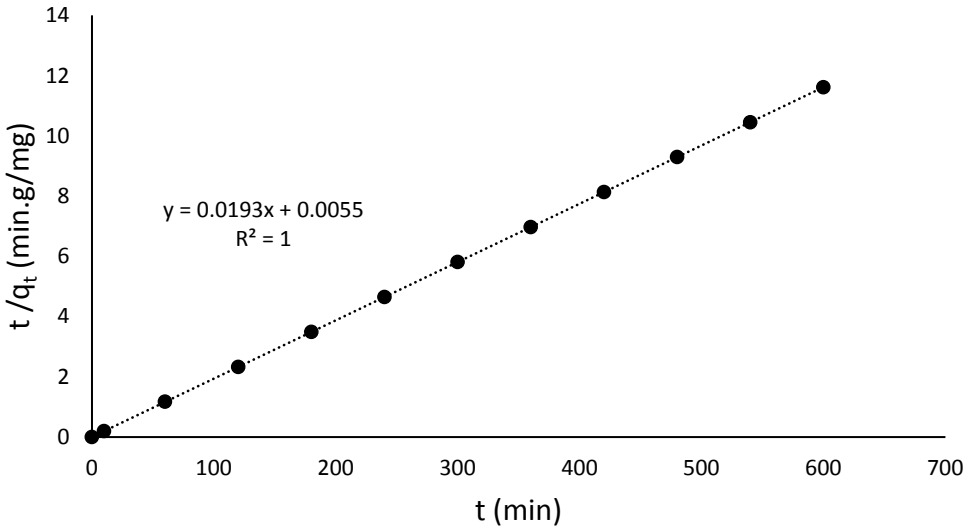

Fig. 8 Pseudo-second-order adsorption kinetic of Co onto the soil

In Fig. 9, the terms 1/ß ln (αß) and 1/ß for Elovich kinetic model are calculated from the intercept and slope of the linear plot of q_t versus ln (t). The value of the correlation coefficient (R^2) of the Elovich model was 0.8741.

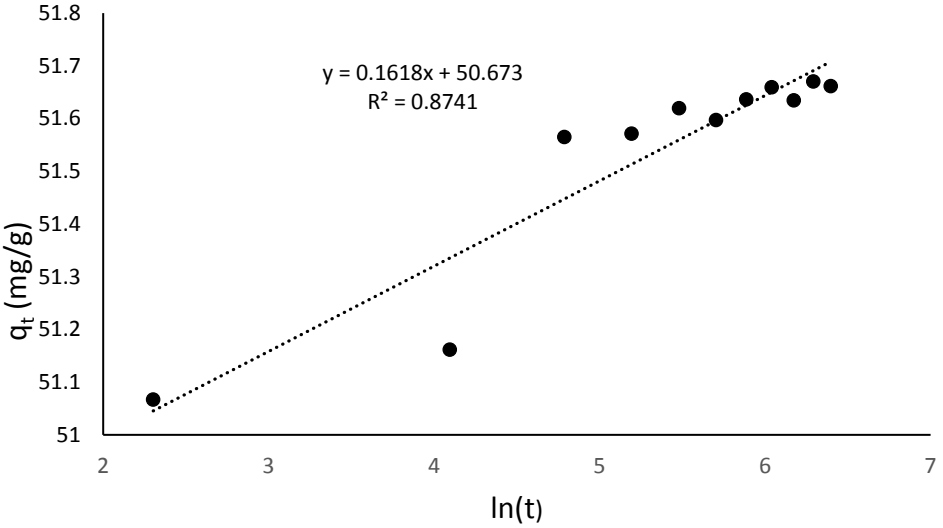

Fig. 9 Elovich adsorption kinetic of Co onto the soil

In terms of rate-limiting regarding the adsorption, the slowest step of the reaction (rate-limiting step) could be the boundary layer (film) or the intra-particle (pore) diffusion of solute from the bulk of the solution on the solid surface in a batch process. A higher value of intercept (I) means a greater influence of the boundary layer. If the plot of q_t versus $t^{0.5}$ becomes a straight line and passes through the origin, the rate-limiting step can be linked to the intra-particle diffusion (Sheela et al. 2012). In Fig. 10, plot deviation from linearity shows the rate limiting step is controlled by the boundary film diffusion. Non-linearity of the plot describes the two or more Co adsorption

steps in soil. This means that intra-particle diffusion might not be the only mechanism, the adsorption rate is controlled by a combination of the two processes (Arabloo et al. 2016). Table 8 presents the correlation and R^2 obtained from applied kinetic models. The coefficient of determination (R^2), k_{id} and intercept (I) calculated from the intra particle kinetic model are 0.7988, 0.0375 and 50.9, respectively.

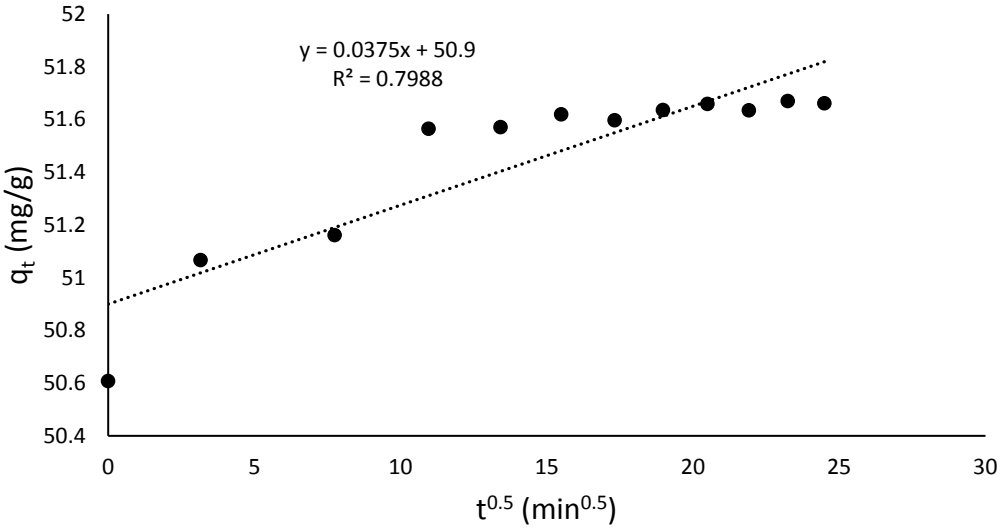

Fig. 10 Intra-particle diffusion adsorption kinetic of Co onto the soil

Table 8 Kinetic models regarding Co adsorption in soil

Kinetic model	Equation	R^2
pseudo-first-order	$\ln(q_e-q_t)= -0.5549- 0.0078t$	0.8427
pseudo-second-order	$t/q_t= 0.0055 + 0.0193t$	1
Elovich	$q_t= 50.673 + 0.1618 \ln(t)$	0.8741
Intra-particle diffusion	$q_t= 0.0375\ t^{0.5} + 50.9$	0.7988

3.5 Isotherm Examination of Co Adsorption in Soil with and without Existence of Biosurfactants

The isotherm models were developed using MATLAB software. Four isotherms, including Redlich-Peterson, Langmuir, Freundlich and Temkin, were discussed. The Redlich-Peterson isotherm is the combination of both the Langmuir and Freundlich equations (Rostamian et al. 2011). The Langmuir isotherm supposes monolayer adsorption onto a homogeneous surface with a limited number of identical sites (Farah et al. 2007). The Freundlich isotherm is chosen to evaluate the intensity of adsorption of sorbent in the particles. The Temkin isotherm, similar to the Freundlich model, is one of the early isotherms. The isotherm models are indicated in Figs. 11-17. Constants and statistical quality measuring of each isotherm model are reported in Tables 9 and 10, respectively. When comparing the values of R^2 and R^2_a obtained from the sorption models without the addition of any biosurfactant, the Freundlich and Redlich-Peterson models had a better performance of fitting the experimental data. However, the Freundlich model has a higher R^2_a (0.9908). If the magnitude of $n > 1$, then the process of adsorption is favorable (Wang et al. 2007).

With no biosurfactant addition, the n value (1.169) from the Freundlich model defined a favorable adsorption process.

When 1 CMC of surfactin was added, the greatest value of R^2 (0.984) was achieved using the Redlich-Peterson model to fit the experimental data. When the surfactin concentration increased to 2 CMC, the greatest value of R^2 (0.9603) was obtained using the Freundlich model. The Freundlich model implies that multilayer adsorption is assumed on the heterogeneous surface, and $n < 0.5$ indicates unfavorable adsorption (Dolatkhah and Wilson 2016). The n value (0.8922) achieved using the Freundlich isotherm indicated a reasonable adsorption.

For trehalose lipids addition at a concentration of 1 CMC and 2 CMC, the Redlich-Peterson isotherm and Temkin isotherm show good performance for fitting the data, respectively. The Temkin model is extracted by simulating that relation between change in the heat of adsorption (ΔH_{ads}) with θ being linear (Rostamian et al. 2011). In terms of the maximum adsorption capacity (Q_0) for the Co adsorption in soil, the Langmuir isotherm (Table 9) resulted in the greatest Q_0 (3.753×10^4 mg/g) in the 1 CMC trehalose lipids system. When using rhamnolipid at 1 and 2 CMC concentrations, the Redlich-Peterson fit the data the best in the 1 CMC system and the Freundlich model was the best in the 2 CMC system. The Redlich-Peterson isotherm resulted in the R^2 values ranging between 0.984 – 0.9936 in all systems, except for the one with an addition of 2 CMC of surfactin.

Table 9 Isotherm parameters for various adsorption isotherms for the adsorption of Co onto the soil

Isotherms	Parameters	No Biosurfactant	1 CMC Surfactin	2 CMC Surfactin	1 CMC Trehalose lipids	2 CMC Trehalose lipids	1 CMC Rhamnolipid	2 CMC Rhamnolipid
Langmuir	Q_0 (mg/g)	381.5	572.3	$3.7*10^4$	$3.753*10^4$	109.1	$1.939*10^4$	39150
	K_l (L/mg)	0.2683	0.03741	0.0005037	0.001648	0.9424	0.0006117	0.0002633
Freundlich	K_f (L/g) $(mg/g)^{nf}$	81.37	21.27	16.45	62.91	49.11	11.76	8.184
	n_f	1.169	1.105	0.8922	0.8916	1.677	0.996	0.8759
Temkin	b_T	1.406	0.0639	0.01201	0.3852	0.1495	3.488	0.04999
	A_T (L/g)	21.68	3.713	1.368	10.48	9.375	1.915	1.079
Redlich-Peterson	K_R (L/g)	33.75	18.24	19.08	55.74	80	11.37	10.32
	a_R (1/mg)	-0.5852	-0.1262	$-3.101*10^6$	-0.117	0.4081	$-9.283*10^{-6}$	1.249
	g	0.1445	-0.906	-30.11	2.668	1.707	5.139	- 47.45

Table 10 Isotherm error deviation data related to the adsorption of Co onto the soil

Isotherms	Error functions	No biosurfactant	1 CMC Surfactin	2 CMC Surfactin	1 CMC Trehalose lipids	2 CMC Trehalose lipids	1 CMC Rhamnolipid	2 CMC Rhamnolipid
Langmuir	R^2	0.9886	0.9806	0.9536	0.9839	0.9811	0.9879	0.9914
	Adjusted R^2	0.9848	0.9742	0.9382	0.9785	0.9749	0.9838	0.9885
Freundlich	R^2	0.9931	0.9822	0.9603	0.9884	0.9427	0.9879	0.9993
	Adjusted R^2	0.9908	0.9763	0.9471	0.9845	0.9236	0.9839	0.9991
Temkin	R^2	0.8774	0.8839	0.6079	0.8353	0.9983	0.8964	0.9301
	Adjusted R^2	0.5095	0.5358	-0.5686	0.3414	0.9931	0.5857	0.7202
Redlich-Peterson	R^2	0.9931	0.984	0.8326	0.9931	0.9918	0.9908	0.9936
	Adjusted R^2	0.9861	0.9679	0.6653	0.9863	0.9835	0.9817	0.9871

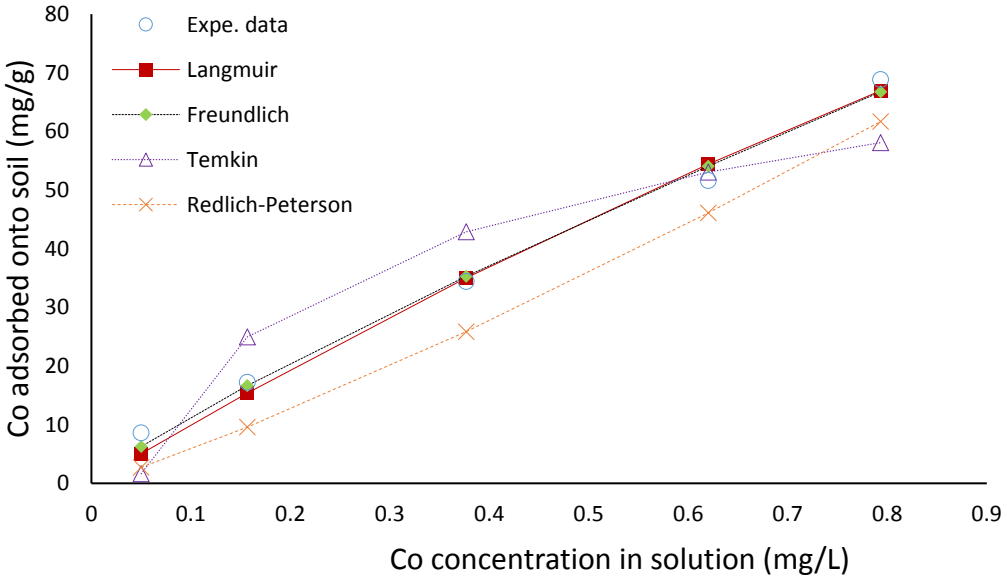

Fig. 11 Comparison of various sorption isotherms for Co onto soil without biosurfactant

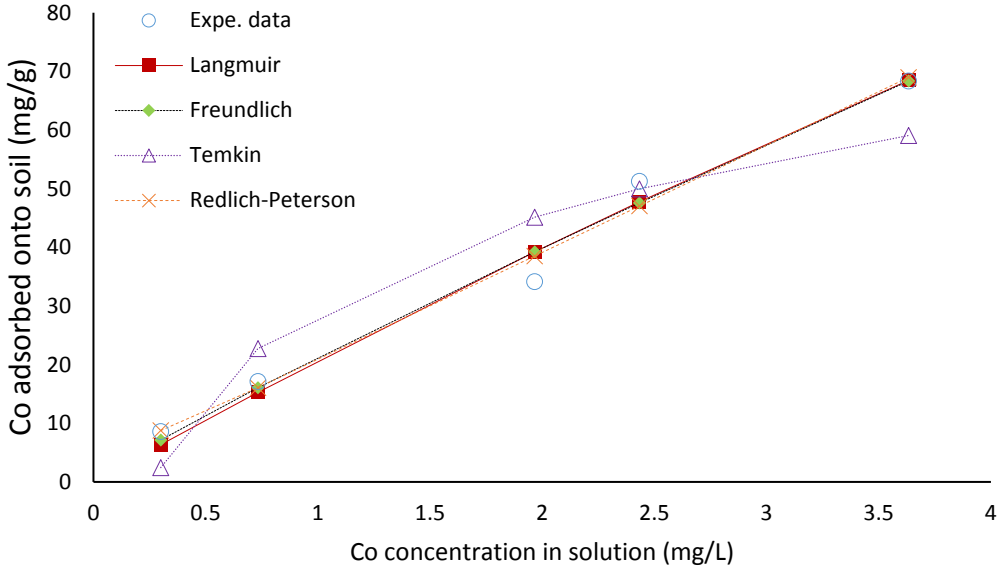

Fig. 12 Comparison of various sorption isotherms for Co onto soil with 1 CMC surfactin

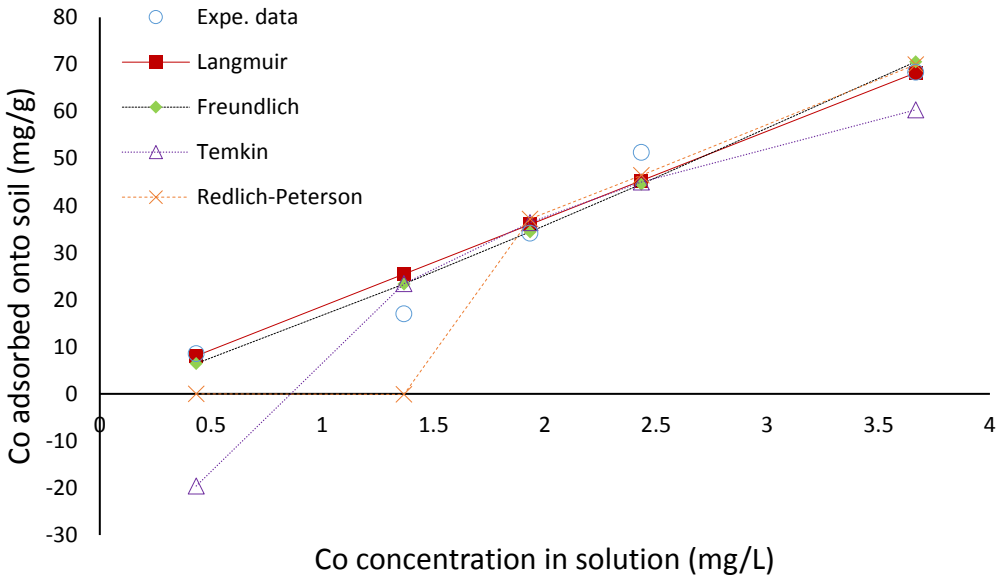

641
642
643 **Fig. 13** Comparison of various sorption isotherms for Co onto soil
644 with 2 CMC surfactin
645

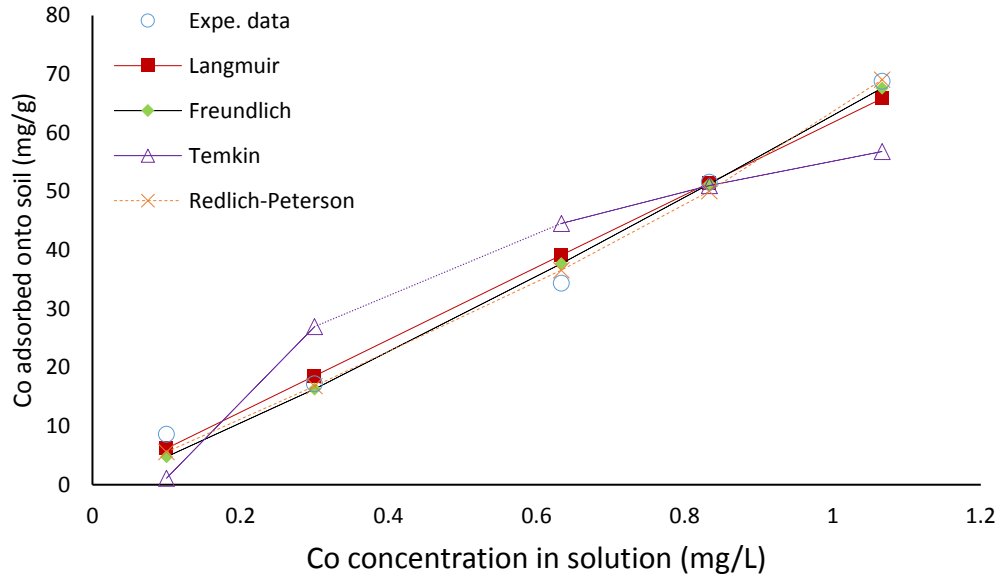

646
647 **Fig. 14** Comparison of various sorption isotherms for Co onto soil
648 with 1 CMC trehalose lipids
649
650

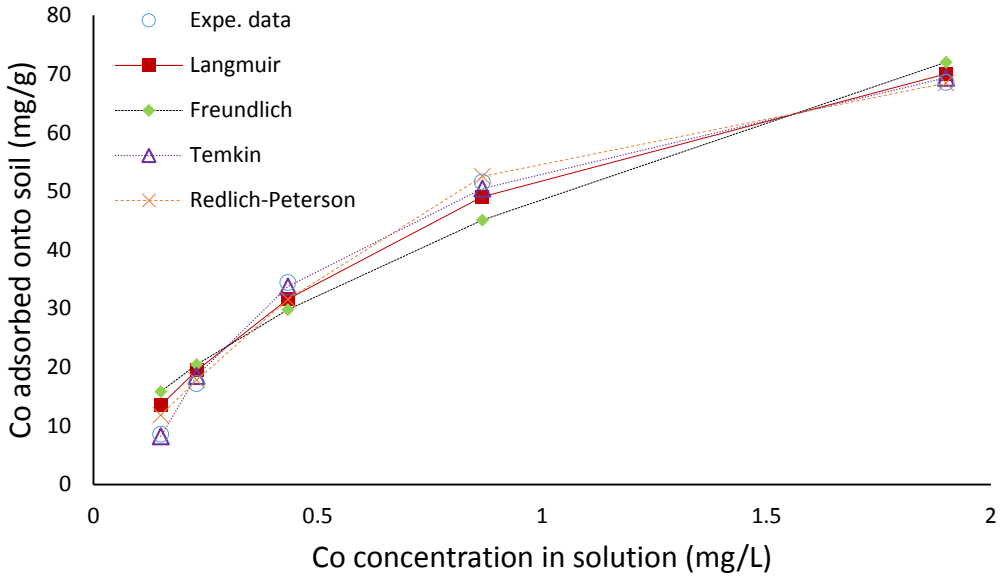

Fig. 15 Comparison of various sorption isotherms for Co onto soil with 2 CMC trehalose lipids

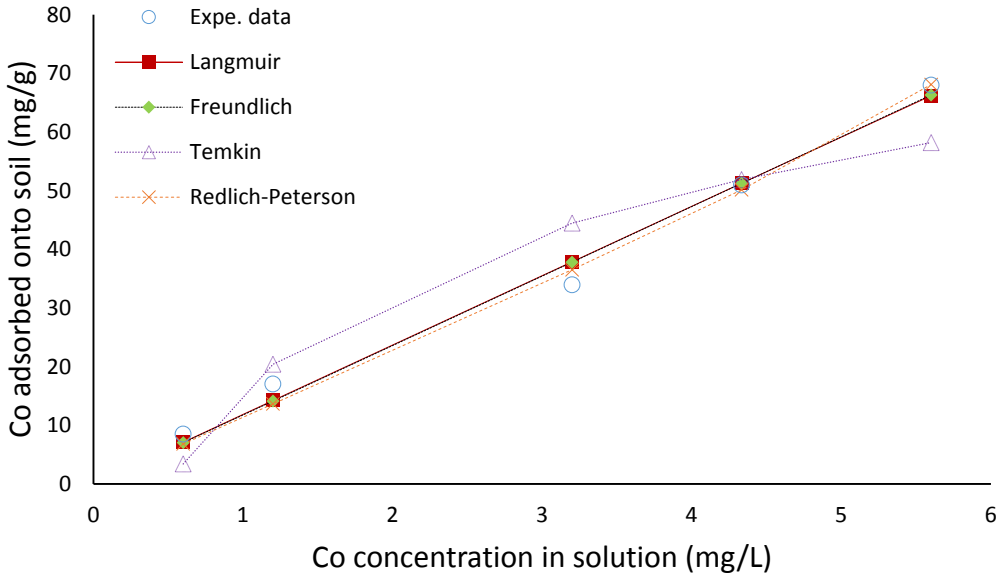

Fig. 16 Comparison of various sorption isotherms for Co onto soil with 1 CMC rhamnolipid

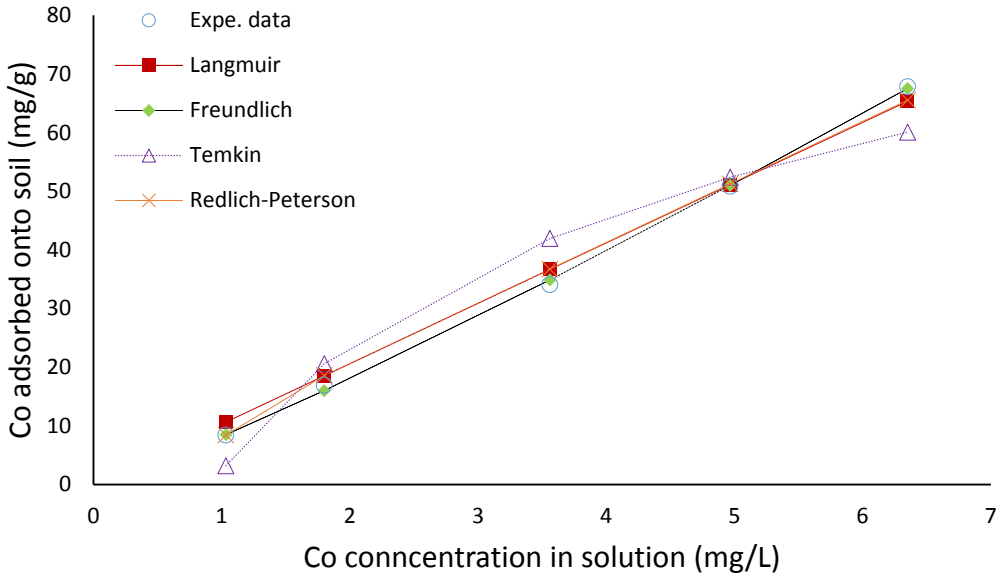

Fig. 17 Comparison of various sorption isotherms for Co onto soil with 2 CMC rhamnolipid

4 Conclusions

In this study, Co adsorption in saline soil with and without the existence of a biosurfactant was examined. The impact of pH, contact time, initial Co concentration, and type/dose of biosurfactant on Co adsorption were evaluated and three biosurfactants including surfactin, trehalose lipids and rhamnolipid products were used. At a low initial concentration of Co, increasing surfactin concentration has a positive impact on the remaining Co in the solution. On the other hand, at a high concentration of Co, the concentration of biosurfactant does not have significant impact on the remaining Co. Surfactin was seen to be weakly sorbed in the soil. Trehalose lipids at any concentration reduced the remaining Co in the solution, compared with surfactin. Studying the adsorption characteristics of Trehalose lipids results in the high capacity of adsorption by the soil. When applying rhamnolipid, by increasing the initial concentration of Co, the remaining Co in the solution increased considerably at any initial concentration of rhamnolipid. The high value range of surface tension of solutions (60-70 mN/m) shows that rhamnnolipid has a high tendency of adsorption to the soil surface.

Adsorption kinetics were also explored. The kinetic parameters were investigated using the pseudo-first-order, pseudo-second-order, as well as the Elovich and intraparticle diffusion rate models. The adsorption kinetic data fit the best in the pseudo-second-order model with the largest regression coefficient (R^2) obtained and the similarity between the Co equilibrium concentration based on model calculation ($q_{e\text{-}cal}$ = 51.8134 mg/g) and on experimental data (q_e = 51.6591 mg/g). The intraparticle diffusion model indicated that boundary layer diffusion affects the adsorption rate.

Langmuir, Freundlich, Temkin and Redlich-Peterson adsorption models were applied for the isotherm investigation. Results indicated that with no biosurfactant addition, the adsorption isotherm was well described by the Freundlich model. In the system with surfactin addition, the Redlich-Peterson and Freundlich models can show the adsorption the best with 1 CMC and 2

CMC, respectively. When using trehalose lipids and rhamnolipid, the best fitting isotherms were the Redlich-Peterson isotherm (1 CMC of trehalose lipids and rhamnolipid), Temkin isotherm (2 CMC of trehalose lipids), and Freundlich isotherm (2 CMC of rhamnolipid), respectively. The highest adsorption of Co (Q_0: 3.753 □ 10^4 mg/g) was achieved when 1 CMC of Trehalose lipids was introduced to the soil.

This study identified that Co has a strong adsorption capacity in low permeable saline soil. The research findings based on the Co adsorption kinetics and isotherms can help to explore the related mechanisms and the impact of biosurfactants on the fate of Co in soil, so as to aid the screening of proper soil remediation technologies.

Acknowledgments

The authors would like to express their gratitude to Canada Research Chairs (CRC) Program, Canada Foundation for Innovation (CFI), Natural Sciences and Engineering Research Council of Canada (NSERC), and Rhamnolipid Inc. for their support.

References

Abbas, M., Kaddour, S., & Trari, M. (2014). Kinetic and equilibrium studies of cobalt adsorption on apricot stone activated carbon. *Journal of Industrial and Engineering Chemistry*, 20, 745–751.

Altintas, Y. (2012). *Manufacturing Automation: Metal Cutting Mechanics, Machine Tool Vibrations, and CNC Design*. Cambridge University Press.

Arabloo, M., Ghazanfari, M. H., & Rashtchian, D. (2016). Wettability modification, interfacial tension and adsorption characteristics of a new surfactant: Implications for enhanced oil recovery. *Fuel*, 185, 199–210.

Aşçi, Y., Nurbaş, M., & Açikel, Y. S. (2007). Sorption of Cd(II) onto kaolin as a soil component and desorption of Cd(II) from kaolin using rhamnolipid biosurfactant. *Journal of Hazardous Materials*, B 139, 50–56.

ASTM (2016a). Standard Test Method for pH of Soils. ASTM D4972-18, ASTM International, ASTM International, West Conshohocken, PA. http://www.astm.org/cgi-bin/resolver.cgi?D4972. Accessed 25 August 2018.

ASTM (2016b). Standard Test Methods for Laboratory Determination of Density (Unit Weight) of Soil Specimens. ASTM D7263-09(2018)e2, ASTM International, West Conshohocken, PA. http://www.astm.org/cgi-bin/resolver.cgi?D7263. Accessed 25 August 2018.

ASTM (2016c). Standard Test Methods for Laboratory Determination of Water (Moisture) Content of Soil and Rock by Mass. ASTM D2216-10, ASTM International, West Conshohocken, PA. http://www.astm.org/cgi-bin/resolver.cgi?D2216. Accessed 25 August 2018.

Cai, Q. (2018). Biosurfactant production and applications in oil contaminate control. PhD thesis. Department of Civil Engineering, Memorial University of Newfoundland, St. John's, NL, Canada.

Cai, Q., Zhang, B., Chen, B., & Cao, T. (2016). Biosurfactant produced by a rhodococcus erythropolis mutant as an oil spill response agent. *Water Quality Research Journal of Canada*, 51(2), 97–105.

737 Cai, Q., Zhang, B., Chen, B., Zhu, Z., Lin, W, & Cao, T. (2014). Screening of biosurfactant
738 producers from petroleum hydrocarbon contaminated sources in cold marine environments.
739 *Marine Pollution Bulletin*, 86(1–2), 402–410.
740 Chen, L., & Lu, S. (2008). Sorption and desorption of radiocobalt on montmorillonite-Effects of
741 pH, ionic strength and fulvic acid. *Applied Radiation and Isotopes*, 66, 288–294.
742 Chon, J. K., Lee, K. J., & Yun, J.-Il (2012). Sorption of cobalt(II) on soil: Effects of birnessite and
743 humic acid. *Journal of Radioanalytical and Nuclear Chemistry*, 293, 511–517.
744 Coleman, N. J., Brassington, D. S., Raza, A., & Mendham, A. P. (2006). Sorption of Co^{2+} and Sr^{2+}
745 by waste-derived 11 Å tobermorite. *Waste Management*, 26, 260–267.
746 Dolatkhah, A., & Wilson, L. D. (2016). Magnetite/Polymer Brush Nanocomposites with
747 Switchable Uptake Behavior Toward Methylene Blue. *ACS Applied Materials and Interfaces*,
748 8, 5595–5607.
749 Ebrahimzadeh Rajaei, G., Aghaie, H., Zare, K., & Aghaie, M. (2013). Adsorption of Cu(II) and
750 Zn(II) ions from aqueous solutions onto fine powder of Typha latifolia L. root: Kinetics and
751 isotherm studies. *Research on Chemical Intermediates*, 39, 3579–3594.
752 Farah, J. Y., El-Gendy, N. S., & Farahat, L. A. (2007). Biosorption of astrazone blue basic dye
753 from an aqueous solution using dried biomass of Baker's yeast. *Journal of Hazardous*
754 *Materials*, 148, 402–408.
755 Faroon, O. M. (2004). Toxicological Profile for Cobalt. U.S. Department of Health and Human
756 Services, Public Health Service, Agency for Toxic Substances and Disease Registry, Atlanta,
757 Georgia. http://www.atsdr.cdc.gov/toxprofiles/tp33.pdf. Accessed 25 August 2018.
758 Ferraro, A., Fabbricino, M., van Hullebusch, E. D., Esposito, G., & Pirozzi, F. (2016). Effect of
759 soil/contamination characteristics and process operational conditions on
760 aminopolycarboxylates enhanced soil washing for heavy metals removal: a review. *Reviews*
761 *in Environmental Science and Biotechnology*, 15, 111–145.
762 Filipkowska, U., & Kuczajowska-Zadrozina, M. (2016). Investigation of the adsorption/desorption
763 equilibria of Cd(II), Zn(II) and Cu(II) ions on/from immobilized digested sludge using
764 biosurfactants. *Environmental Earth Sciences*, 75, 814.
765 Freitas de Oliveira, D. W., França, I. W., Félix, A. K., Martins, J. J., Giro, M. E., Melo, V. M., &
766 Gonçalves, L. R. (2013). Kinetic study of biosurfactant production by Bacillus subtilis
767 LAMI005 grown in clarified cashew apple juice. *Colloids and Surfaces B: Biointerfaces*, 101,
768 34–43.
769 Guerra, D. L., & Airoldi, C. (2008). Anchored thiol smectite clay-kinetic and thermodynamic
770 studies of divalent copper and cobalt adsorption. *Journal of Solid State Chemistry*, 181, 2507–
771 2515.
772 Harendra, S., & Vipulanandan, C. (2013). Sorption and transport studies of cetyl
773 trimethylammonium bromide (CTAB) and Triton X-100 in clayey soil. *Journal of*
774 *Environmental Sciences*, 25(3), 576–584.
775 Hashemian, S., Saffari, H., & Ragabion, S. (2015). Adsorption of cobalt(II) from aqueous solutions
776 by Fe3O4/bentonite nanocomposite. *Water, Air, and Soil Pollution*, 226, 2212.
777 Ho, Y. S., & McKay, G. (1999). Pseudo-second order model for sorption processes. *Process*
778 *Biochemistry*, 34, 451–465.
779 Jalali, M., & Majeri, M. (2016). Cobalt sorption-desorption behavior of calcareous soils from some
780 Iranian soils. *Chemie der Erde*, 76, 95–102.
781 Komy, Z. R., Shaker, A. M., Heggy, S. E. M., & El-Sayed, M. E. A. (2014). Kinetic study for
782 copper adsorption onto soil minerals in the absence and presence of humic acid.

Chemosphere, 99, 117–124.
Meitei, M. D., & Prasad, M. N. V. (2013). Lead (II) and cadmium (II) biosorption on Spirodela polyrhiza (L.) Schleiden biomass. *Journal of Environmental Chemical Engineering*, 1, 200–207.
Mulligan, C. N., Yong, R. N., & Gibbs, B. F. (2001). Surfactant-enhanced remediation of contaminated soil: A review. *Engineering Geology*, 60, 371–380.
Najafi, M., Rostamian, R., & Rafati, A. A. (2011). Chemically modified silica gel with thiol group as an adsorbent for retention of some toxic soft metal ions from water and industrial effluent. *Chemical Engineering Journal*, 168, 426–432.
Naqvi, A. H., Hunt, A., Burnett, B. R., & Abraham, J. L. (2008). Pathologic spectrum and lung dust burden in giant cell interstitial pneumonia (hard metal disease/cobalt pneumonitis): Review of 100 cases. *Archives of Environmental and Occupational Health*, 63(2), 51–70.
Pérez-Marín, A. B., Zapata, M., Ortuño, J. F., Aguilar, M., Sáez, J., & Lloréns, M. (2007). Removal of cadmium from aqueous solutions by adsorption onto orange waste. *Journal of Hazardous Materials*, 139(1), 122–131.
Rostamian, R., Najafi, M., & Rafati, A. A. (2011). Synthesis and characterization of thiol-functionalized silica nano hollow sphere as a novel adsorbent for removal of poisonous heavy metal ions from water: Kinetics, isotherms and error analysis. *Chemical Engineering Journal*, 171, 1004–1011.
Sheela, T., Nayaka, Y. A., Viswanatha, R., Basavanna, S., & Venkatesha, T. G. (2012). Kinetics and thermodynamics studies on the adsorption of Zn(II), Cd(II) and Hg(II) from aqueous solution using zinc oxide nanoparticles. *Powder Technology*, 217, 163–170.
Siddiqui, Z., Jawaid, S. M. A., Vishen, S., & Verma, Sh. (2015). Remediation of Heavy Metals Contaminated Soil and Soil Washing. i-manager's Journal on Civil Engineering, 5(3), 1-6.
Singh, A. K., & Cameotra, S. S. (2013). Efficiency of lipopeptide biosurfactants in removal of petroleum hydrocarbons and heavy metals from contaminated soil. *Environmental Science and Pollution Research*, 20, 7367–7376.
Siva Kumar, N., Woo, H. S., & Min, K. (2012). Equilibrium and kinetic studies on biosorption of 2,4,6-trichlorophenol from aqueous solutions by Acacia leucocephala bark. *Colloids and Surfaces B: Biointerfaces*, 94, 125–132.
Smičiklas, I., Onjia, A., Raičević, S., Janaćković, Đ., & Mitrić, M. (2008). Factors influencing the removal of divalent cations by hydroxyapatite. 152, 876–884.
Srivastava, V. C., Mall, I. D., & Mishra, I. M. (2006). Equilibrium modelling of single and binary adsorption of cadmium and nickel onto bagasse fly ash. *Chemical Engineering Journal*, 117, 79–91.
Tong, K. S., Kassim, M. J., & Azraa, A. (2011). Adsorption of copper ion from its aqueous solution by a novel biosorbent Uncaria gambir: Equilibrium, kinetics, and thermodynamic studies. *Chemical Engineering Journal*, 170, 145–153.
Wang, X.-S., Huang, J., Hu, H.-Q., Wang, J., & Qin, Y. (2007). Determination of kinetic and equilibrium parameters of the batch adsorption of Ni(II) from aqueous solutions by Na-mordenite. *Journal of Hazardous Materials*, 142(1-2), 468–476.
WHO (2007). IARC Monographs on the Evaluation of Carcinogenic Risks to Humans, Vol. 90 Human papillomaviruses, World Health Organization International Agency for Research on Cancer, Lyon, France. https://monographs.iarc.fr/wp-content/uploads/2018/06/mono90.pdf. Accessed 25 August 2018.
Zhu, Z., Zhang, B., Chen, B., Cai, Q., & Lin, W. (2016). Biosurfactant Production by Marine-

Originated Bacteria Bacillus Subtilis and Its Application for Crude Oil Removal. *Water, Air, and Soil Pollution*, 227, 328.